Development of nanocomposites for anode materials in Li-ion batteries

Rolf Ochs[1], **Dorothée Vinga Szabó**[*,1], **Sabine Schlabach**[1], **Sebastian Becker**[2], **and Sylvio Indris**[2]

[1] Institute for Materials Research III, Karlsruhe Institute of Technology, Hermann von Helmholtz Platz 1, 76344 Eggenstein Leopoldshafen, Germany
[2] Institute of Nanotechnology, Karlsruhe Institute of Technology, Hermann von Helmholtz Platz 1, 76344 Eggenstein Leopoldshafen, Germany

Keywords core/shell particles, *in situ* deposition, Li ion batteries, nanoparticles, SnO_2, tin dioxide

[*] Corresponding author: e mail dorothee.szabo@kit.edu, Phone: +49 7247 82 2938, Fax: +49 7247 82 3956

Nanocomposites based on SnO_2 with carbon scaffold were used as highly porous anode films on Ni substrates. The films were obtained by *in situ* deposition of the particles without any binder or excess carbon black avoiding any secondary treatment. Compared to similarly prepared uncoated SnO_2 nanoparticles as well as conventionally prepared powder samples the capacity loss of the *in situ* deposited nano composite films is significantly reduced. Thus, this newly developed anode material combined with *in situ* film formation is a promising approach for high capacity anodes in Li ion batteries.

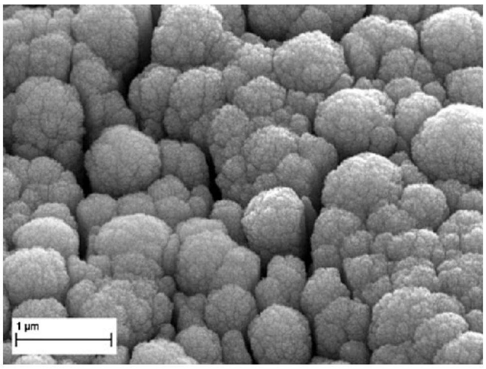

SEM micrograph of a SnO_2/C nanoparticle film.

1 Introduction The growing demand of high capacity Li-ion batteries for automotive or stationary energy applications creates a need for new and improved electrode materials. Nanostructured conversion materials like tin dioxide (SnO_2) or silicon (Si) possess very promising potential as anode material in Li-ion batteries [1] because they exhibit in many cases much higher specific capacities than currently used carbon anodes. SnO_2, for instance, features theoretical specific capacities of 782 mAh/g [2] which are more than twice as high as for currently used carbon anodes with 372 mAh/g [2, 3]. Bulk conversion materials however show very poor long-term cycle stability due to internal stress caused by the large volume change ($SnO_2 > 200\%$) and crack formation [1] during the (dis-) charging process. One possibility to address this issue is the use of nanocomposites consisting of core/shell nanoparticles with an active core, e.g. SnO_2, and a stabilizing shell, e.g. carbon, which acts as a scaffold between the core particles. Such materials could also benefit from their nanoporous morphology featuring local free space to compensate volume change. In the present study we demonstrate improved cycle stability of porous films made of core/shell nanoparticles without excess carbon black and binder compared to similarly prepared but uncoated SnO_2 nanoparticles as well as conventionally prepared powder samples using a binder and secondary doctor blading.

2 Experimental SnO_2 nanoparticles as well as nanocomposites based on this oxide and carbon have been synthesized utilizing the Karlsruhe Microwave Plasma Process (KMPP), a gas-phase synthesis method described elsewhere [4]. For the utilization as negative electrode material in Li-ion batteries the nanocomposite particles have been deposited *in situ* as a nanoparticle film on Ni-Substrates according to the method described in previous work [5]. As precursor for the core particles tin-tetrachloride ($SnCl_4$), and for the carbon shell 1,3-Dicyclopentadiene ($C_{10}H_{12}$) were employed. The relevant synthesis parameters used in the context of this work were precursor feeding rates 5 ml/h of $SnCl_4$, 5 ml/h of dicyclopentadiene for a thick coating, 1 ml/h of dicyclopentadiene for a thin coating, gas flow (20% O_2 in Ar) of 5 l/min, microwave power of 600 W for the core particles (first reaction stage) and 340 W for the shell (second reaction stage), preheat time of 5 min and coating time of the substrates of 15 min. In a typical run 4 ml of $SnCl_4$ and appropriate amounts of dicyclopentadiene were used.

Microstructural characterization was carried out on additionally collected powder by transmission electron microscopy (TEM) in a FEI Tecnai F20ST at 200 kV equipped with a Gatan Imaging Filter. For TEM sample preparation nanoparticles were deposited on 300 mesh Cu grids covered with holey carbon films by dipping the grid into the powder. The morphology and the thickness of the *in situ* deposited nanoparticle layers were analysed using a scanning electron microscope (Zeiss Supra-55).

All test cells were assembled in an Ar-filled glove box (M. Braun, Unilab, Germany) using a Li metal counter electrode, a porous separator, and an electrolyte of 1 M $LiPF_6$ solution in a 1:1 mixture of ethylene carbonate (EC) and dimethyl carbonate (DMC). The *in situ* deposited nanoparticle films (SnO_2 and core/shell SnO_2/C) were directly assembled in Swagelock cells, without any carbon black or binder. The content of active material (SnO_2) was 1.4 mg for SnO_2, and 0.6 mg for SnO_2/C with thick coating, respectively. For comparison, powder samples of SnO_2 nanoparticles, synthesized under similar conditions, were mixed with 10 wt.% carbon black and 10 wt.% polyvinylidene fluoride (PVDF) as binder, and a slurry was made with N-methyl-2-pyrrolidon (NMP). The slurry was used to coat 0.02-mm thick copper foils with a 120 μm doctor blade. This film was dried for 24 h at 80 °C. The foils were cut into circular pieces of 12 mm diameter and assembled in coin type test cells (CR2032), containing 2.83 mg of active material. Electrochemical cell testing between 0.02 and 2.8 V was done using an Arbin Instruments battery testing system.

3 Results and discussion

Transmission electron microscopy of the so produced particles (Fig. 1) shows a relatively uniform particle or core size of about 5 nm. The shape of the particles is typically spherical.

The characterization of the carbon shell of the SnO_2/C nanocomposites is much more elaborate. In case of the thin coating (Fig. 1a) the shell is difficult to detect. This difficulty results mainly from the fact that the carbon coating is assumed to be thinner than the resolution of the microscope (0.24 nm). Additionally, it is amorphous and provides only weak interaction with the e beam due to the low atomic number. In case of the thick coating (Fig. 1b) the shell is clearly visible but it is not possible to determine a well-defined thickness of this shell. Anyhow, even the thin carbon coating can be detected clearly using electron energy loss spectroscopy (EELS) which is shown in Fig. 2. Comparing the low loss spectrum with reference spectra of amorphous carbon and bulk SnO_2, carbon identification is not easily done. However, the carbon signal is clearly visible in the core losses. As the spectra were acquired on sample areas lying over holes of the grid covering holey carbon film, the carbon signal definitely stems from the sample, and not from the carbon film. Complementary gravimetric determination of

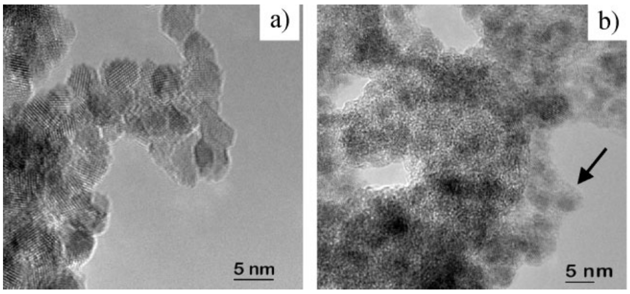

Figure 1 TEM: Bright field image of SnO_2/C nanoparticles. (a) Thin coating, lattice fringes of SnO_2 are visible, carbon shell is difficult to detect. (b) Thick coating, carbon shell is clearly visible (arrows).

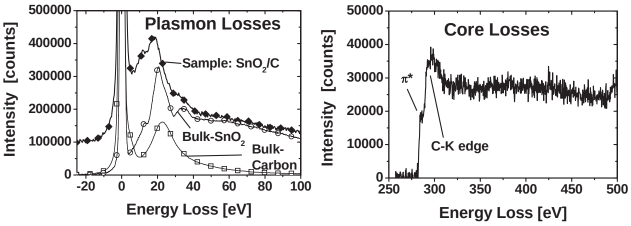

Figure 2 Electron energy loss spectra of SnO_2/C core/shell nanoparticles with thin carbon shell. For better visibility, the plasmon loss spectra are stacked. The bulk spectra herein show reference spectra to clarify the peak positions. The presence of the carbon coating can be proved in the core losses.

Figure 3 (online colour at: www.pss a.com) Electron diffraction pattern of SnO_2 nanoparticles. The inset shows a line profile of the diffraction image, visualising the intensity distribution. Peak positions and Miller's indices for the tetragonal cassiterite structure, based on JCPDS 41 1445, are given.

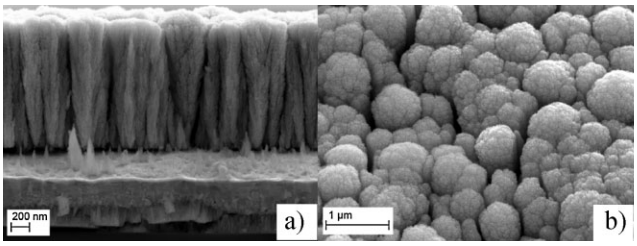

Figure 4 SEM: (a) In-plane view of SnO_2 nanoparticle layer with club-like morphology. b) Top view of the SnO_2/C layer.

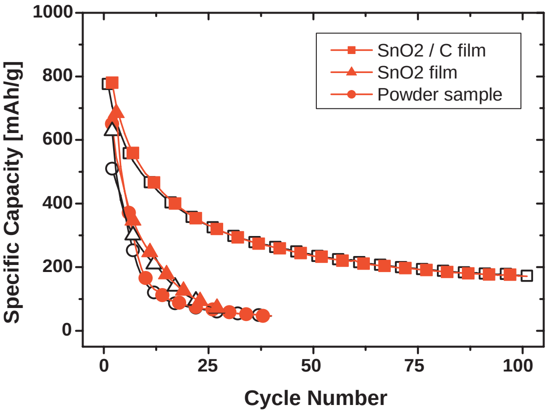

Figure 5 (online colour at: www.pss-a.com) Charge (black open symbols) and discharge (red closed symbols) capacity of different SnO_2 nanoparticle electrodes versus cycle number. Comparison of an *in situ* deposited film of C-coated SnO_2 particles with thick C shell, an *in situ* deposited film of uncoated SnO_2 particles, as well as a conventionally powder processed sample.

carbon content yields 16.7 wt.% for the thin, and 63.5 wt.% for the thick coating, respectively.

The crystal structure of the SnO_2 particles is identified by electron diffraction to be the tetragonal cassiterite structure (Fig. 3). The peak broadening in the diffraction pattern also indicates a crystallite size of around 5 nm.

SEM characterization of the *in situ* deposited nanoparticle films reveals in all cases a highly porous, club-like morphology, as shown in Fig. 4. The thickness of the films was between 1 and 2 µm. The produced nanoparticle films showed a quite good mechanical stability up to a thickness of several µm, verified by tape tests. The actual porosity or accessible surface of these films was not measured, but surface measurements according to Brunauer, Emmet and Teller (BET) of comparable powder samples reveal specific surfaces in the region of 100–200 m^2/g which is compatible to particles in the 5 nm range.

In Fig. 5 the specific capacity of different SnO_2 nanoparticle electrodes is shown versus cycle number. The first discharge step, where the irreversible reaction $SnO_2 + 4\,Li \rightarrow Sn + 2\,Li_2O$ takes place, is not shown. The first reversible specific capacity was determined for all samples in the region of about 780 mAh/g, showing a good agreement with the theoretical value. This means at least for the first reversible cycle that all the deposited material is accessible for the Li-ions, i.e. contributes to the storage capacity. With increasing cycle number the capacity drops for all samples. This capacity loss is attributed to internal stress caused by the large volume change during the alloying process from Li and Sn to $Li_{22}Sn_5$ resulting in cracks and loss of active material. The most drastic capacity drop is observed for the conventionally powder processed sample. The capacity of the electrodes made with *in situ* deposited uncoated particles decreases also, but not as fast as for the powder sample. The capacity fading of the electrodes made with *in situ* deposited C-coated particles is least pronounced. Thus, it was possible to retain 50% capacity after 25 cycles and 25% after 100 cycles. Though not yet sufficiently stable for technical applications, the observed cycle stability is in the range of typical tin-based materials [6–9] but without the need of any binder and secondary treatment.

4 Conclusion

Our results show that it is important to use, on the one hand, highly porous materials and, on the other hand, a conductive coating around the single particles acting as a scaffold or glue. Optimizing the shell in terms of thickness and morphology should further enhance the cycle stability. Further investigations and improvements need to be done on this topic.

The concept of a stabilizing shell around single particles combined with an *in situ* deposited porous nanoparticle layer on electrode substrates without any binder and excess carbon black can be easily extended to other conversion materials like Si and to other shell materials like TiO_2. This concept therefore might enable high capacity electrodes in Li-ion batteries.

References

[1] P. G. Bruce, B. Scorsati, and J. M. Tarascon, Angew. Chem. Int. Ed. **47**, 2930 (2008).
[2] C. Wang, Y. Zhou, M. Ge, X. Xu, Z. Zhang, and J. Z. Jiang, J. Am. Chem. Soc. **132**, 46 (2010).
[3] T. Ozhuku, Y. Iwakoshi, and R. Sawai, J. Electrochem. Soc. **140**, 2496 (1993).
[4] D. Vollath and D. V. Szabó, J. Nanopart. Res. **8**, 417 (2006).
[5] B. Schumacher, R. Ochs, H. Tröße, S. Schlabach, M. Bruns, D. V. Szabó, and J. Haußelt, Plasma Process. Polym. **4**, 865 (2007).
[6] Y. Wang and J. Y. Lee, J. Power Sources **144**, 220 (2005).
[7] Y. Liang, J. Fan, X. Xia, and Z. Jia, Mater. Lett. **61**, 4370 (2007).
[8] M. Park, Y. M. Kang, J. H. Kim, G. X. Wang, S. X. Dou, and H. K. Liu, Carbon **46**, 35 (2008).
[9] K. E. Aifantis, S. Brutti, S. A. Hackneya, T. Sarakonsria, and B. Scrosati, Electrochim. Acta **55**, 5071 (2010).

Empfohlene Zitierung:

Ochs, R.; Szabo, D. V.; Schlabach, S.; Becker, S.; Indris, S.
Development of nanocomposites for anode materials in Li-ion batteries
2011. Physica status solidi / A, 208.
doi: 10.5445/IR/110082135

Zitierung der Originalveröffentlichung:

Ochs, R.; Szabo, D. V.; Schlabach, S.; Becker, S.; Indris, S.
Development of nanocomposites for anode materials in Li-ion batteries
2011. Physica status solidi / A, 208, 471–473.
doi:10.1002/pssa.201026652